Materials and Methods

Materials

$PbBr_2$ (99.9%) was purchased from Macklin. PbI_2 (99%) and oleic acid (OA, 90%) were purchased from Heowns. Formamidine Hydrochloride (FACl, 98%) and Formamidine Bromide (FABr, 99.5%) were purchased from Adamas. N, N-dimethylformamide (DMF, 99.9%) and n-Hexane (98%) were purchased from Aladdin. Oleylamine (OAm, 90%) and Acetonitrile (99.9%) were purchased from Energy Chemical. Dichloromethane was purchased from Sinopharm Chemical. Polysulfone (98%, M.W ~80000) was purchased from Meryer. SLC1717 and LC756 were bought from the Nanjing Ningcui Optical Technology Co., Ltd. Chiral dopant *R*-5011, *S*-5011 and *R*-811 were bought from the Nanjing Sanjiang New Materials R & D Co., Ltd. The PDMS elastomer (Sylgard®184) was purchased from Dow Corning. All the reagents and solvents were used as received without any further purification.

Characterization

Photoluminescence, radioluminescence, CPRL and reflection spectra were recorded on a HORIBA iHR-550 spectrometer. The XRD patterns were measured on a BRUKER D8 ADVANCE X-ray diffractometer. The UV-vis absorption spectra of perovskite were recorded on a Rayleigh UV-2200 UV-vis spectrometer. TEM and HRTEM characterization were performed using JEM-F200. CPL spectra together with g_{lum} values were measured and recorded at room temperature on a JASCO CPL-300 spectrophotometer. CD spectra were measured on a JASCO J-1500 spectrophotometer. POM images were recorded on a Nexcope NE620 microscope.

Synthesis

$FAPbClBr_2$ nanocrystals: FACl (8.0 mg, 0.1 mmol) and $PbBr_2$ (36.7 mg, 0.1 mmol) were dissolved in 1 mL DMF forming 0.1 mM solution. Then, 200 μL OA and 15 μL OAm were added. Next, 100 μL of this mixture was injected into 3 mL of chloroform. Nanocrystals were formed within seconds as a colorless solution. For purification, obtained nanocrystal solution was precipitated once with 3 mL of acetonitrile mixture followed by centrifugation at 8000 rpm for 5 min.

$FAPbBr_3$ nanocrystals: FABr (12.5 mg, 0.1 mmol) and $PbBr_2$ (36.7 mg, 0.1 mmol) were dissolved in 1 mL DMF forming 0.1 mM solution. Then, 200 μL OA and 20 μL OAm were added. The remaining experimental procedures followed $FAPbClBr_2$ nanocrystals.
$FAPbBrI_2$ nanocrystals: FABr (12.5 mg, 0.1 mmol) and PbI_2 (46.1 mg, 0.1 mmol) were dissolved in 1 mL DMF forming 0.1 mM solution. Then, 200 μL OA and 25 μL OAm were added. The remaining experimental procedures followed $FAPbClBr_2$ nanocrystals.

Fabrication of perovskite nanoscintillator film: In a typical experiment, 30 mg of $FAPbBr_3$ nanocrystals were dissolved in 0.3 mL chloroform. After sonicating for 10 minutes, 30 mg of polysulfone was added. The mixture was sonicated for another 5 hours to ensure that $FAPbBr_3$ nanocrystals and polysulfone were well mixed. The viscous solution was carefully coated on the quartz plates to get the $FAPbBr_3$@polysulfone film. The $FAPbClBr_2$@polysulfone film and $FAPbBrI_2$@polysulfone film were obtained via the same process.

X-ray image collection: Commercial camera (Alpha 7IV SONY) was used to take images for the X-ray imaging screens. The ISO, aperture, and shutter were set at 1000, 6.3, and 15 s for samples excited by X-ray (dose rate:11.89 μGy s^{-1}).

Fabrication of the *R*/*S*-architecture: In a typical experiment, a liquid crystal cell with a 20 μm cell gap are homemade. Two cleaning quartz were bonded by UV-curable adhesive (irradiating with a UV light for 20 s), spaced with a 20-μm-thick polyimide film. SLC1717 (10 mg), *R*/*S*-5011 and dichloromethane (3 mL) were added to a 5 mL sample bottle. The doping concentration were 3.38%, 2.89% and 2.39%. After ultrasonic treatment for 5 min, the mixture was heated and dried in a vacuum oven at 80 °C to obtained doped CLCs. Then, the CLCs was loaded into a liquid crystal cell by capillary action, and the liquid crystal cell was sealed with the UV-curable adhesive. Finally, the *R*/*S*-architecture was fabricated by depositing the $FAPbBr_3$@polysulfone film onto one quartz of a liquid crystal cell.

Fabrication of patterned chiral nanoscintillators: In a typical experiment, firstly, 300 mg $FAPbBr_3$ nanocrystals solution (10 mL n-hexane) was added into 15 mg of Sylgard 184 component B (curing agent) with stirring. After vacuum treatment at 40 °C for 1 h to remove solvent, the mixture was further added into 135 g of Sylgard 184 component A (silicone elastomer prepolymer). Then the pattern, "the left wing of a butterfly", was fabricated on a liquid crystal cell surface via a two-step screen printing technique. Finally, a "butterfly" pattern displaying a green left wing under X-ray irradiation could be prepared in a vacuum desiccator at 70 °C overnight. The "butterfly" pattern displaying a red right wing under X-ray irradiation was obtain via the similar process.

Figures

Figure S1. Photographs of $FAPbClBr_2$, $FAPbBr_3$ and $FAPbBrI_2$ perovskite nanocrystals in n-hexane under 365 nm UV excitation.

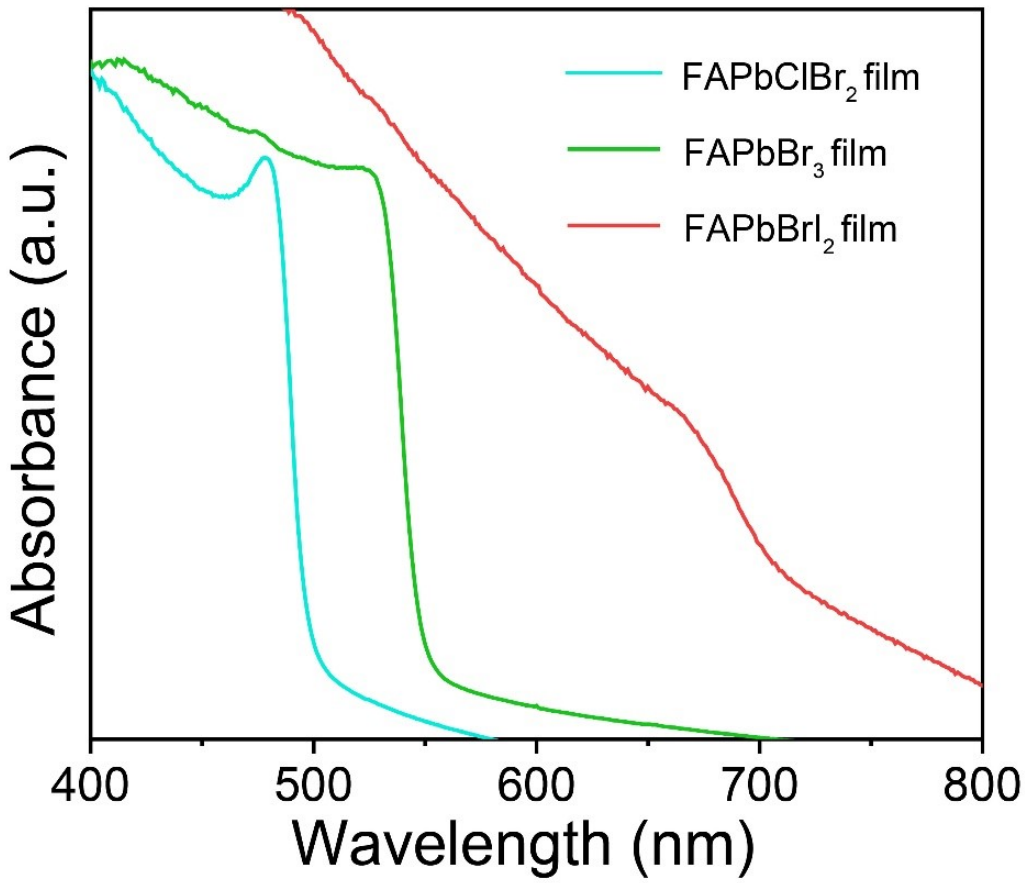

Figure S2. UV-Vis absorption spectra of $FAPbClBr_2$, $FAPbBr_3$ and $FAPbBrI_2$ perovskite nanocrystal films.

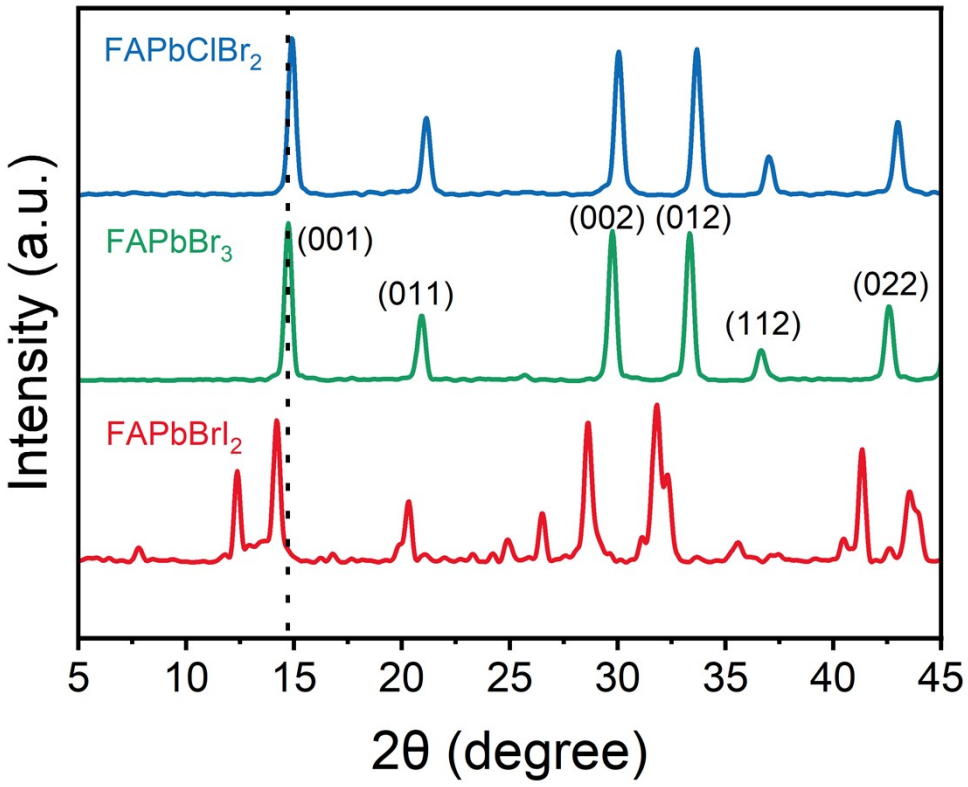

Figure S3. XRD spectra of $FAPbClBr_2$, $FAPbBr_3$ and $FAPbBrI_2$ nanocrystals.

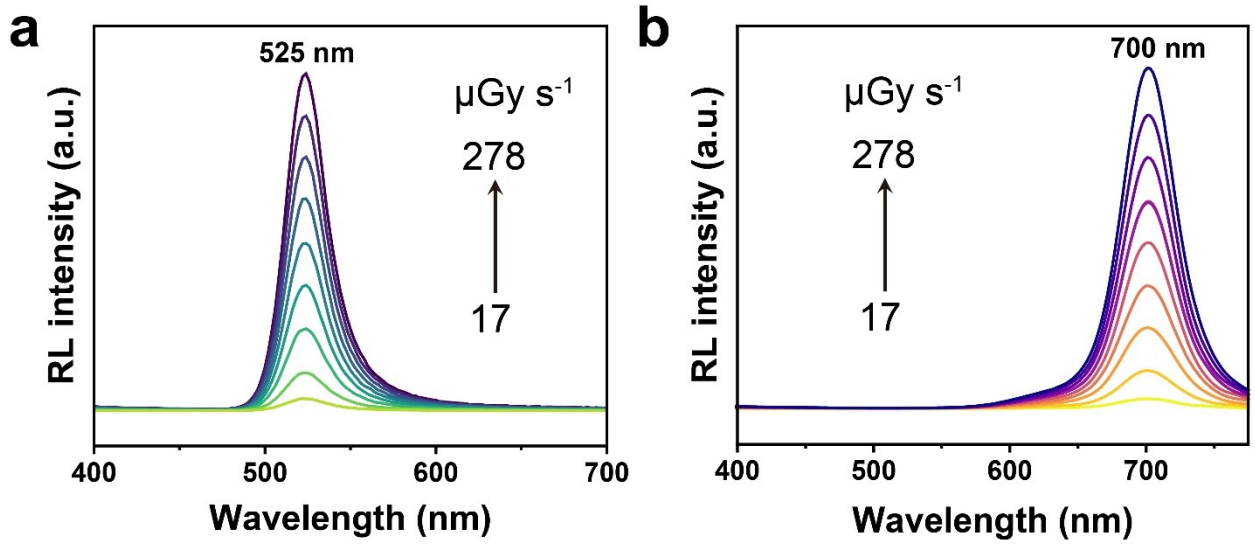

Figure S4. Radioluminescence spectra of (a) $FAPbClBr_2$@polysulfone and (b) $FAPbBrI_2$@polysulfone film under different X-ray dose rates.

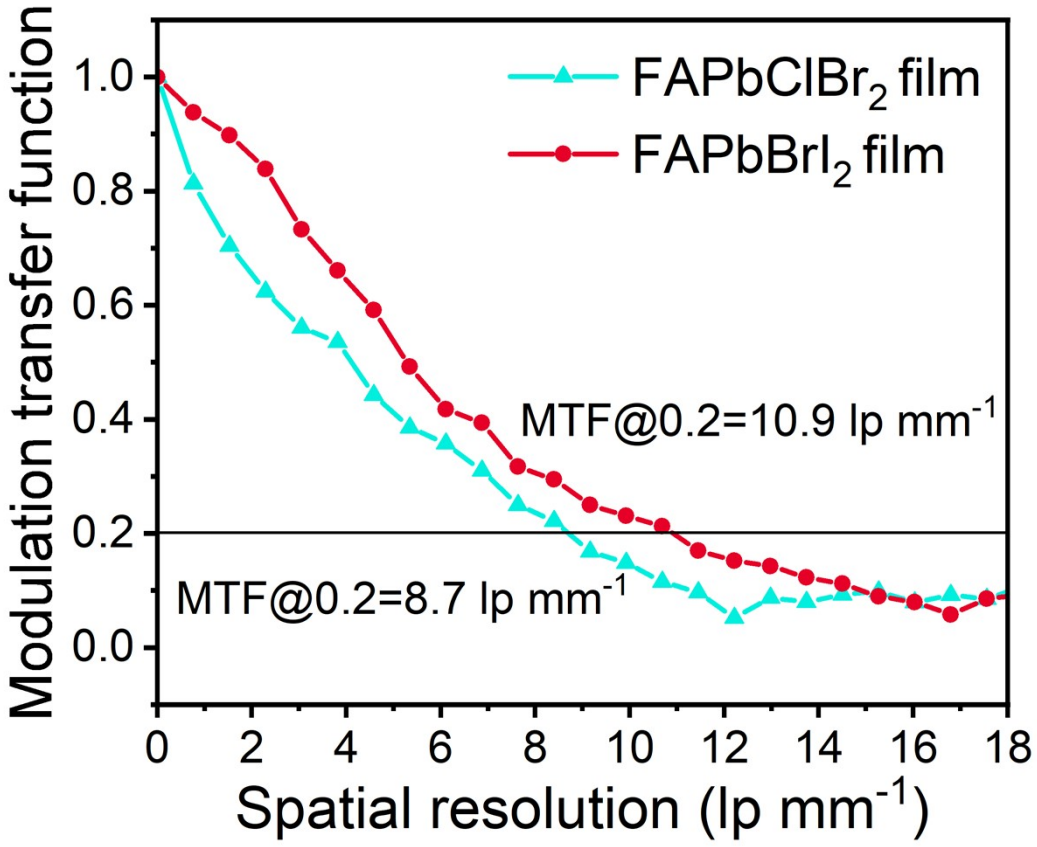

Figure S5. MTFs of X-ray imaging obtained from $FAPbClBr_2$@polysulfone and $FAPbBrI_2$@polysulfone film.

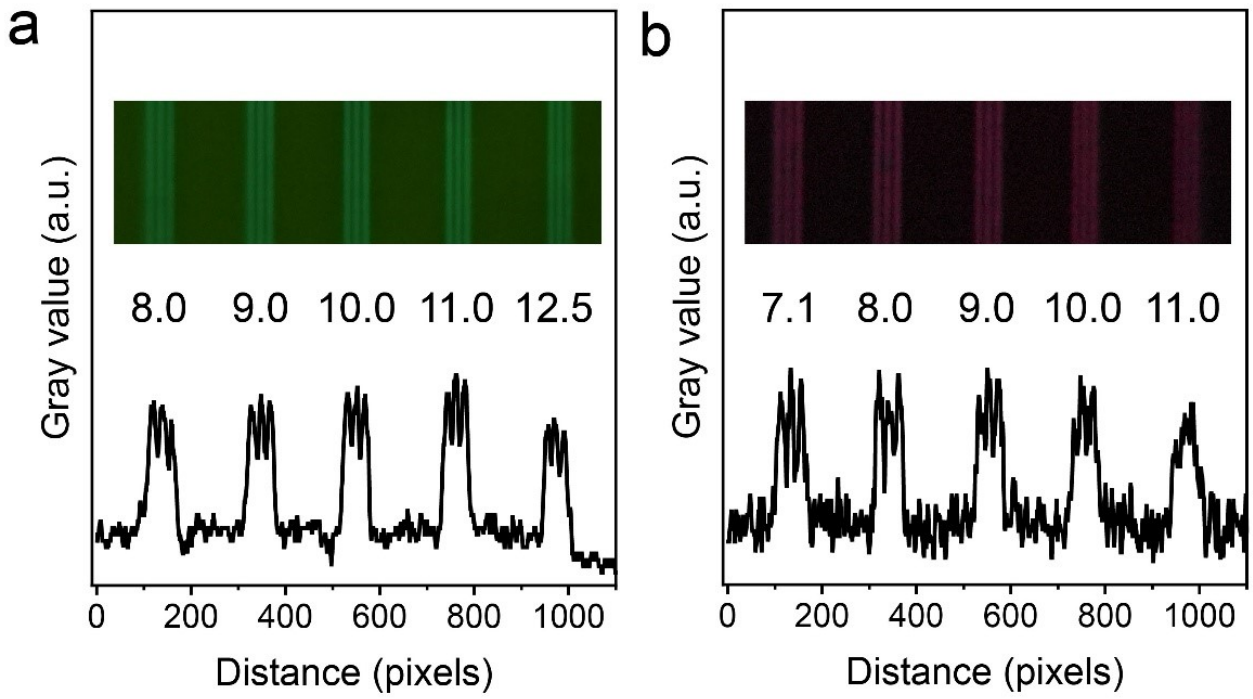

Figure S6. X-Ray image of a standard line-pair card obtained from $FAPbClBr_2$@polysulfone and $FAPbBrI_2$@polysulfone film.

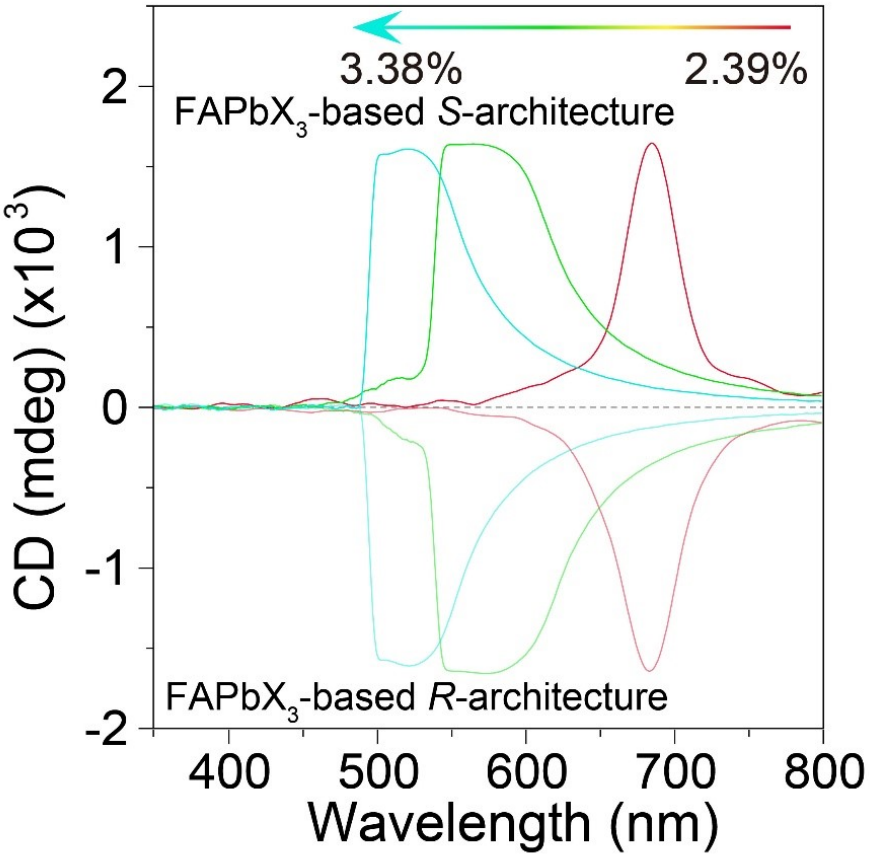

Figure S7. CD spectra of $FAPbClBr_2$, $FAPbBr_3$ and $FAPbBrI_2$-based *S*- and *R*-architecture.

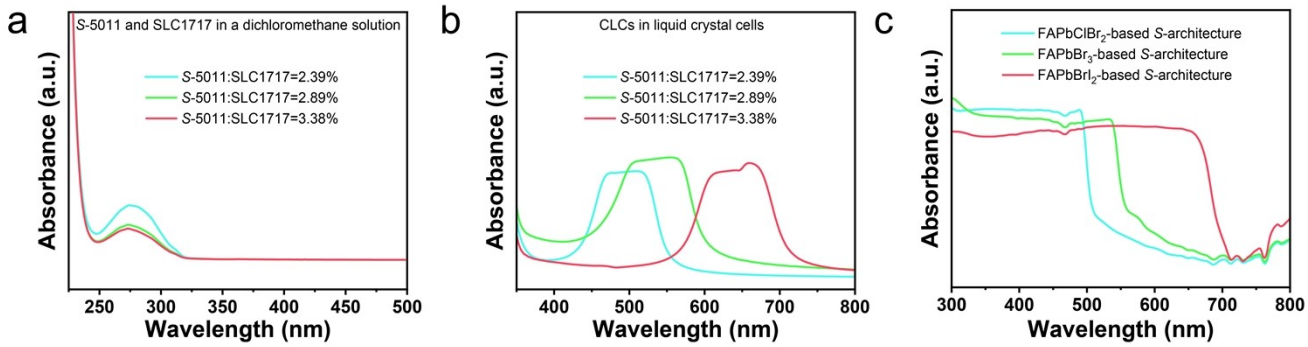

Figure S8. (a) UV-Vis absorption spectra of *S*-5011 and SLC1717 in dichloromethane solution. (b) UV-Vis absorption spectra of CLCs in the liquid crystal cells. (c) UV-Vis absorption spectra of $FAPbClBr_2$, $FAPbBr_3$ and $FAPbBrI_2$-based *S*-architecture.

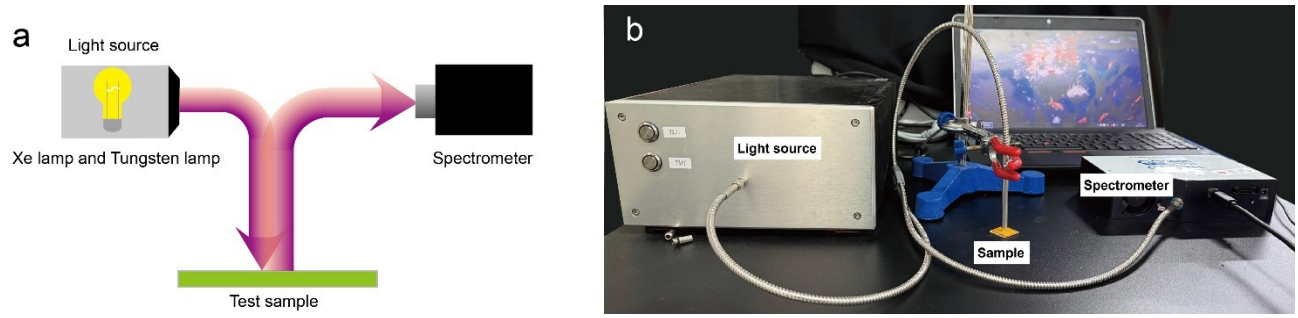

Figure S9. (a) Schematic diagram and (b) photograph of the optical path for reflection spectroscopy measurement.

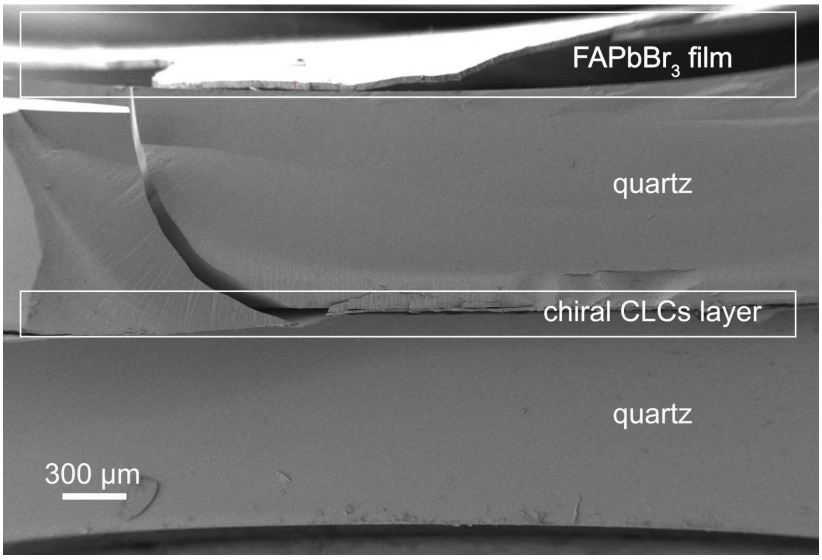

Figure S10. Cross-sectional SEM image of $FAPbBr_3$-based *R*-architecture.

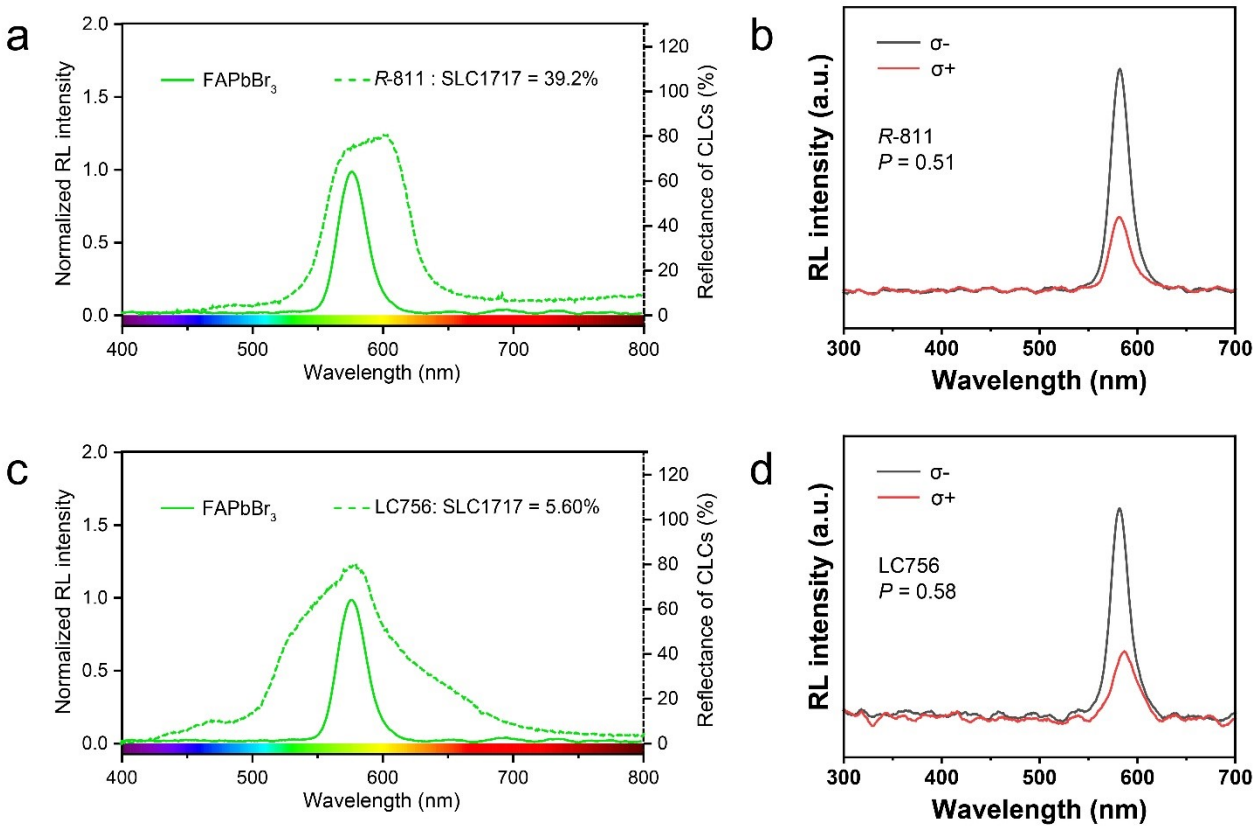

Figure S11. Substitution of the chiral dopant. (a) Reflection spectra of SLC1717 with 39.2% *R*-811 (dashed line) and the radioluminescence spectra of $FAPbBr_3$@polysulfone film (solid line). (b) Polarization-resolved radioluminescence spectra of $FAPbBr_3$-based *R*-811-architecture. (c) Reflection spectra of SLC1717 with 5.60% LC756 (dashed line) and the radioluminescence spectra of $FAPbBr_3$@polysulfone film (solid line). (b) Polarization-resolved radioluminescence spectra of $FAPbBr_3$-based LC756-architecture.

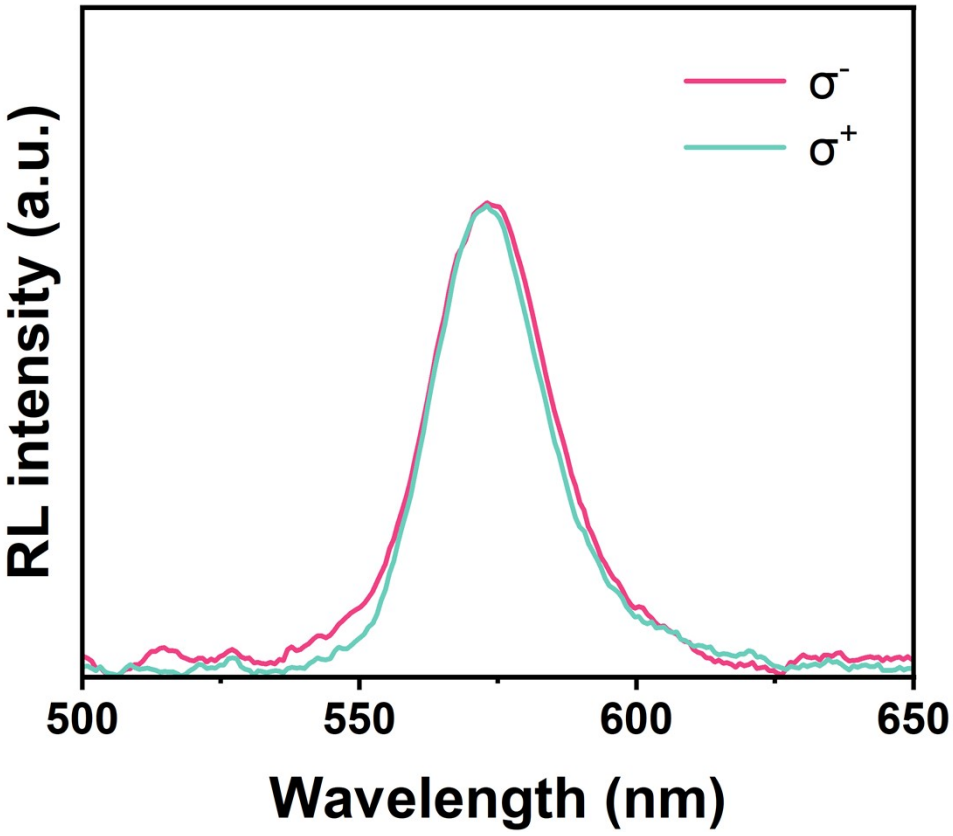

Figure S12. CPRL of achiral $FAPbBr_3$@polysulfone film without chiral CLCs excited by X-ray.

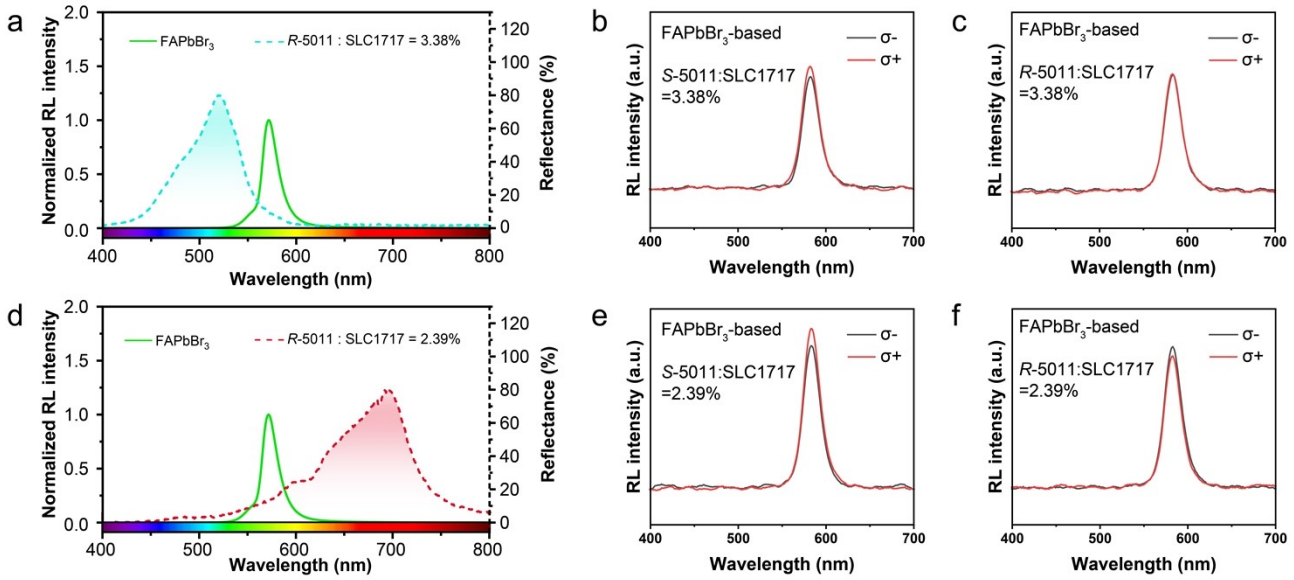

Figure S13. (a) Reflection spectra of SLC1717 with 3.38% *R*-5011 (dashed line) and radioluminescence spectra of $FAPbBr_3$@polysulfone film (solid line). Polarization-resolved radioluminescence spectra of $FAPbBr_3$-based (b) *S*-5011 and (c) *R*-5011 3.38% architecture. (d) Reflection spectra of SLC1717 with 2.39% *R*-5011 (dashed line) and radioluminescence spectra of $FAPbBr_3$@polysulfone film (solid line). Polarization-resolved radioluminescence spectra of $FAPbBr_3$-based (e) *S*-5011 and (f) *R*-5011 2.39% architecture**.**

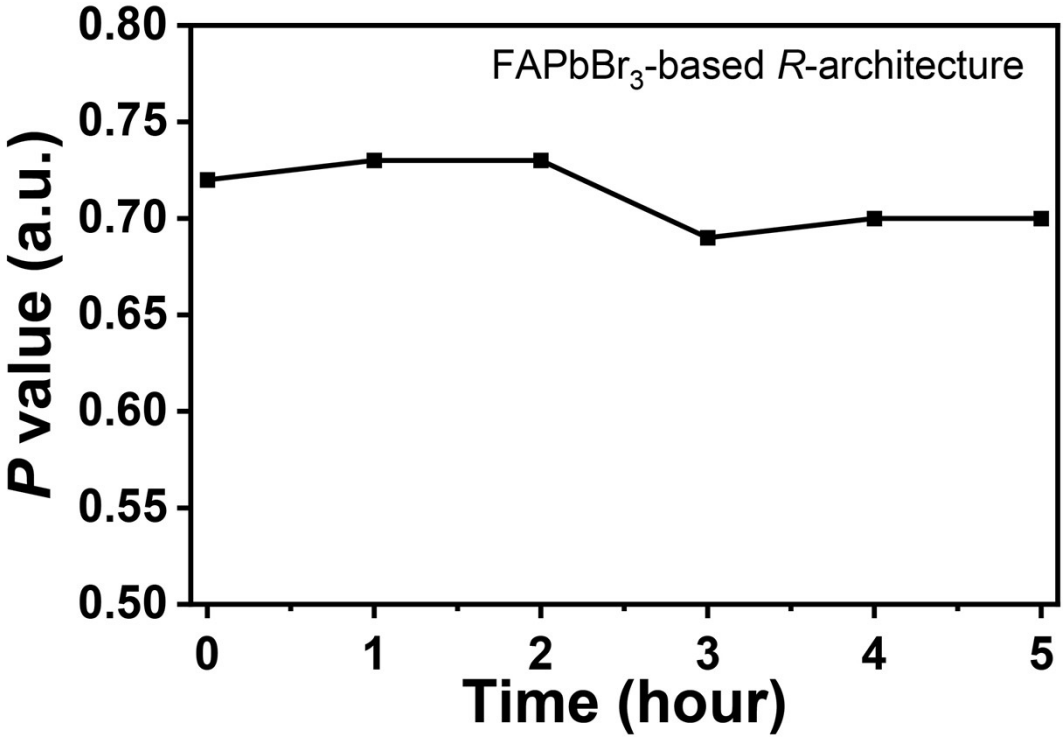

Figure S14. Variation in *P* values under air exposure lasting for 5 h.

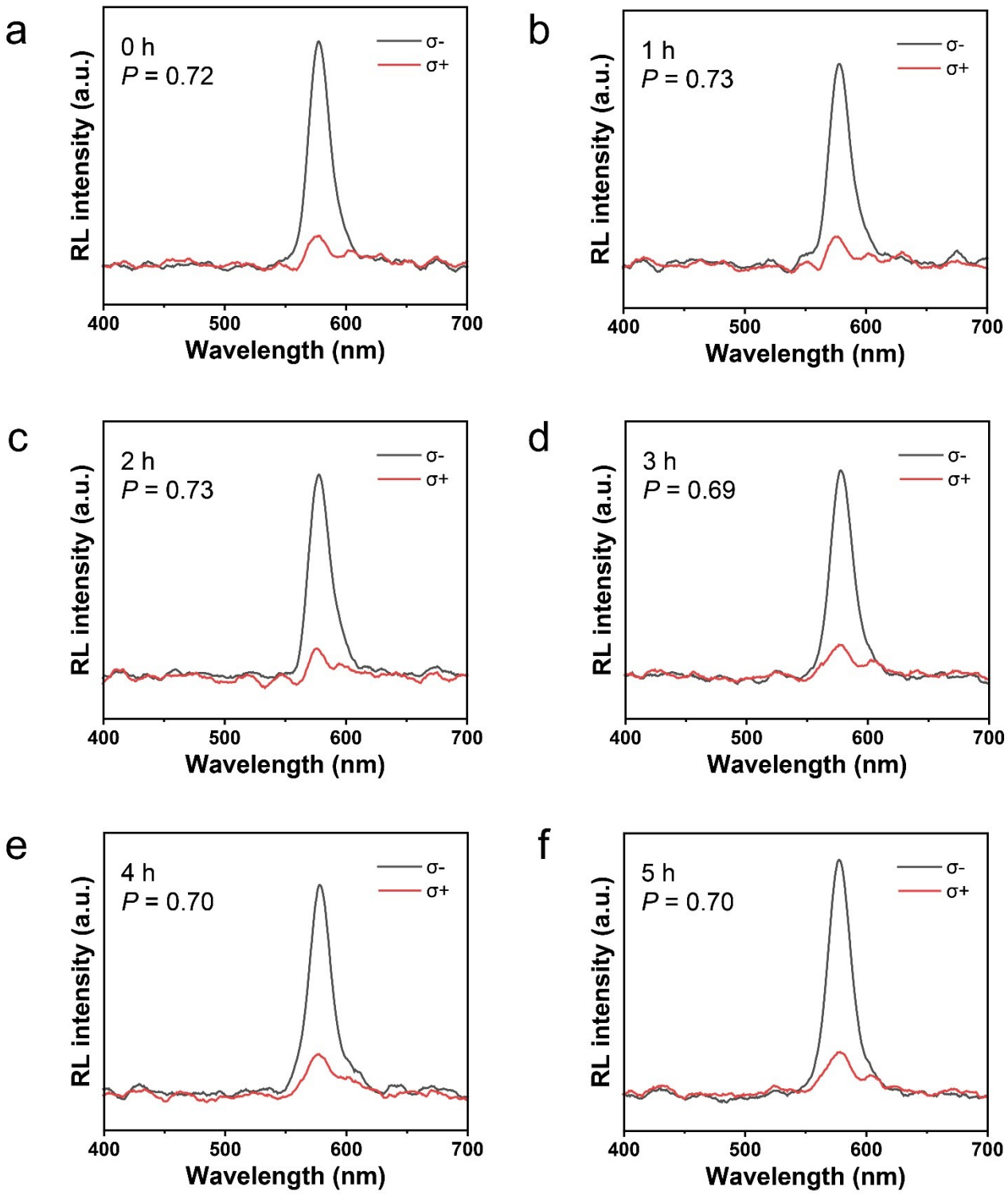

Figure S15. Polarization-resolved radioluminescence spectra of $FAPbBr_3$-based *R*-architecture under air exposure lasting for (a) 0 h, (b) 1 h, (c) 2 h, (d) 3 h, (e) 4 h and (f) 5 h under air exposure.

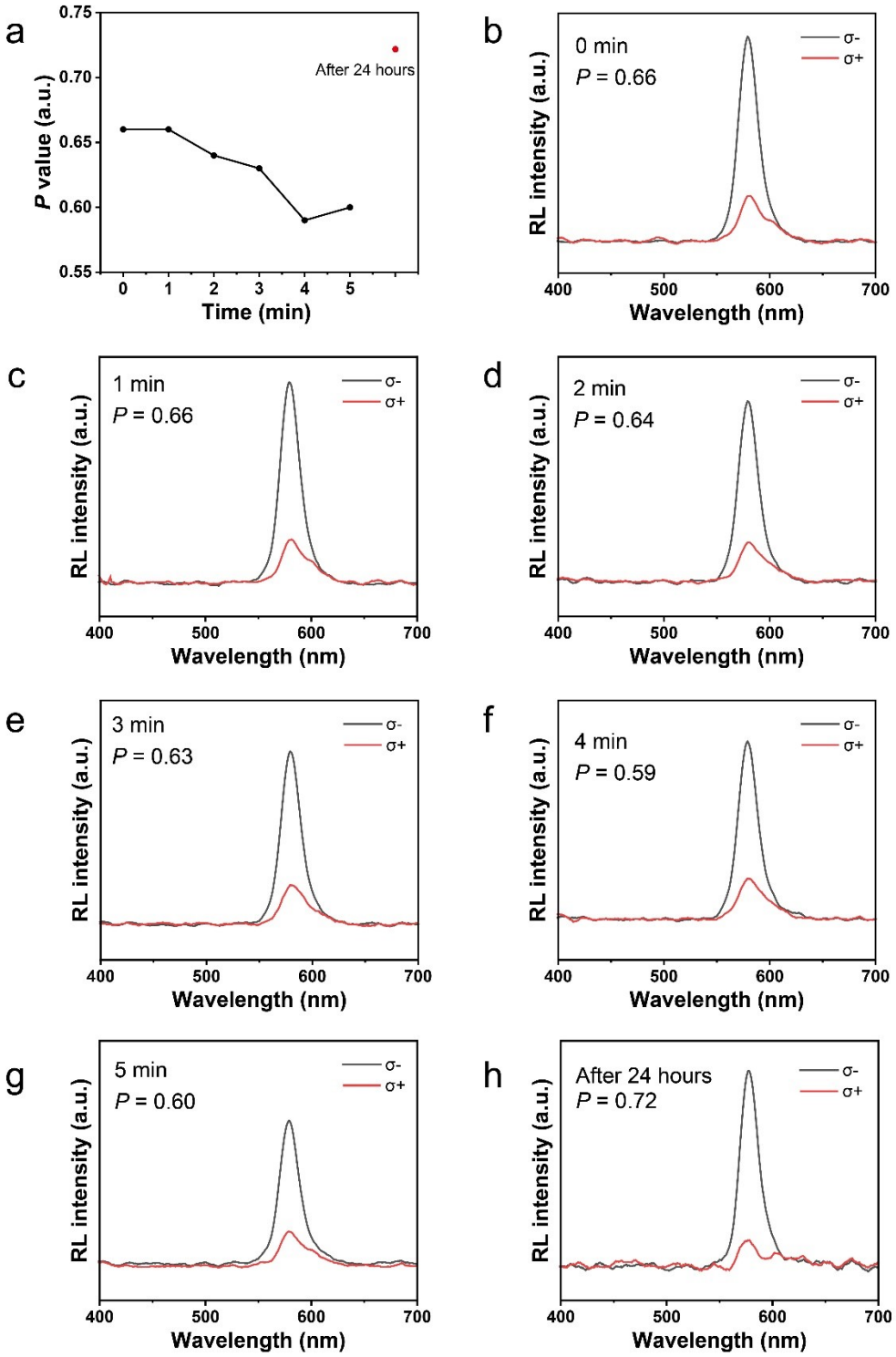

Figure S16. (a) Variation in *P* values of $FAPbBr_3$-based *R*-architecture as a function of continuous X-ray irradiation lasting for 5 minutes. (b-g) Polarization-resolved radioluminescence spectra of $FAPbBr_3$-based *R*-architecture under continuous X-ray irradiation lasting for 0-5 min. (h) Polarization-resolved radioluminescence spectra of $FAPbBr_3$-based *R*-architecture at 24 hours following the completion of irradiation.

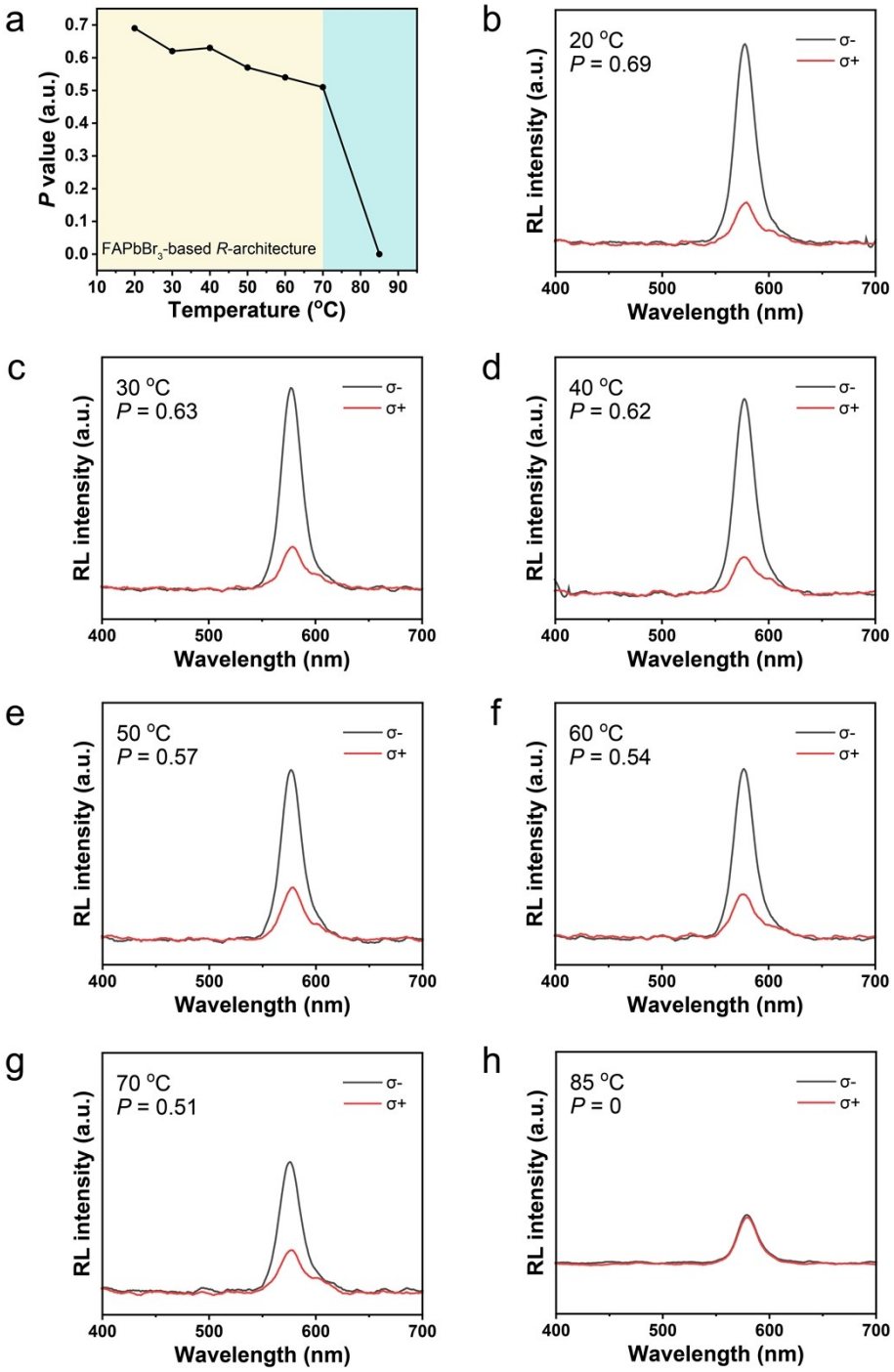

Figure S17. (a) Variation in *P* values of $FAPbBr_3$-based *R*-architecture as a function of temperature. The clearing point of chiral LC is 85°C. (b-h) Polarization-resolved radioluminescence spectra of $FAPbBr_3$-based *R*-architecture under different temperature.

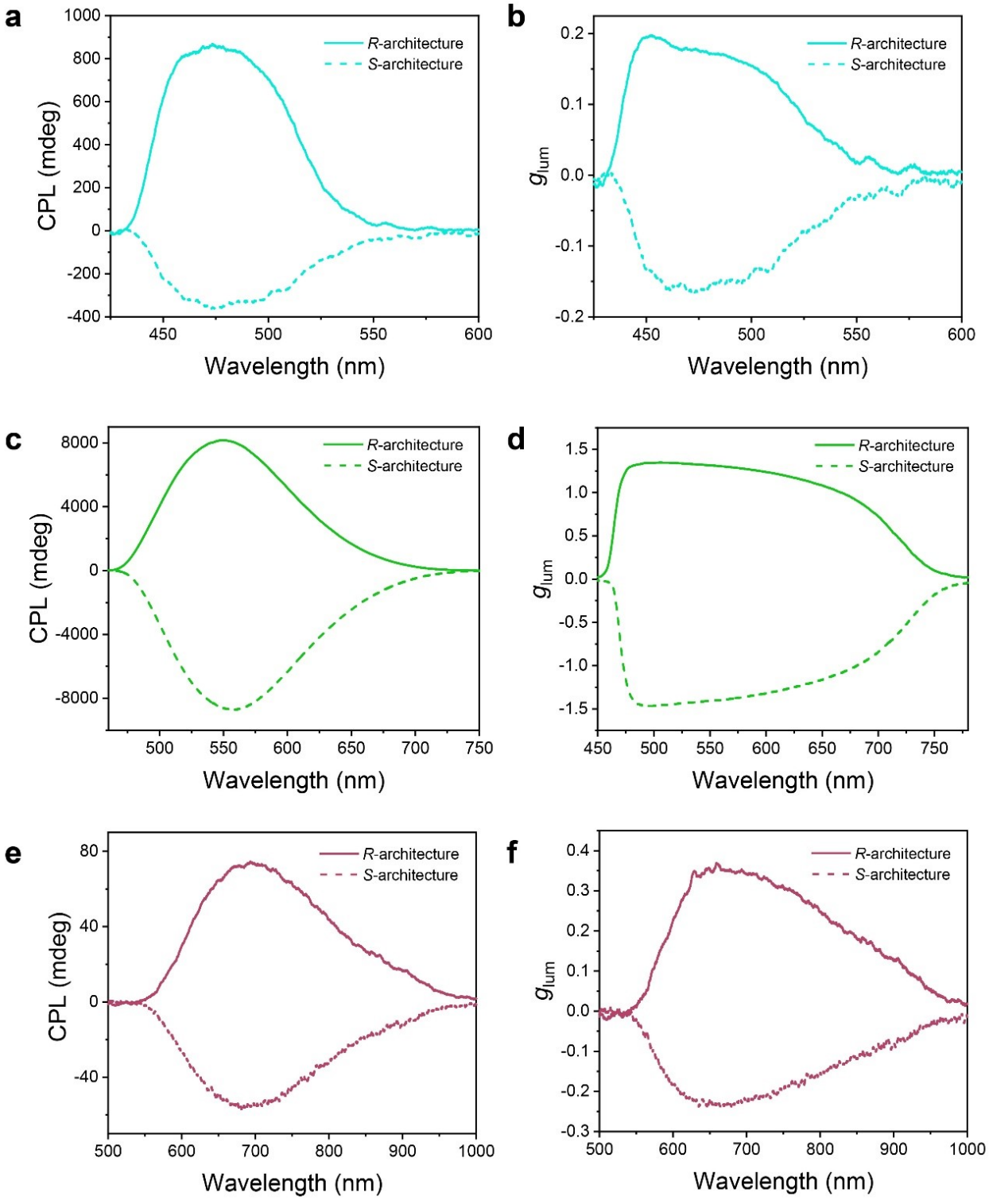

Figure S18. In a typical experiment, CPL spectra of *R*/*S*-architecture based on (a, b) $FAPbClBr_2$, (c, d) $FAPbBr_3$ and (e, f) $FAPbBrI_2$ perovskite nanocrystals conducted on commercial JASCO CPL-300 spectrometer excited by Xe lamp.

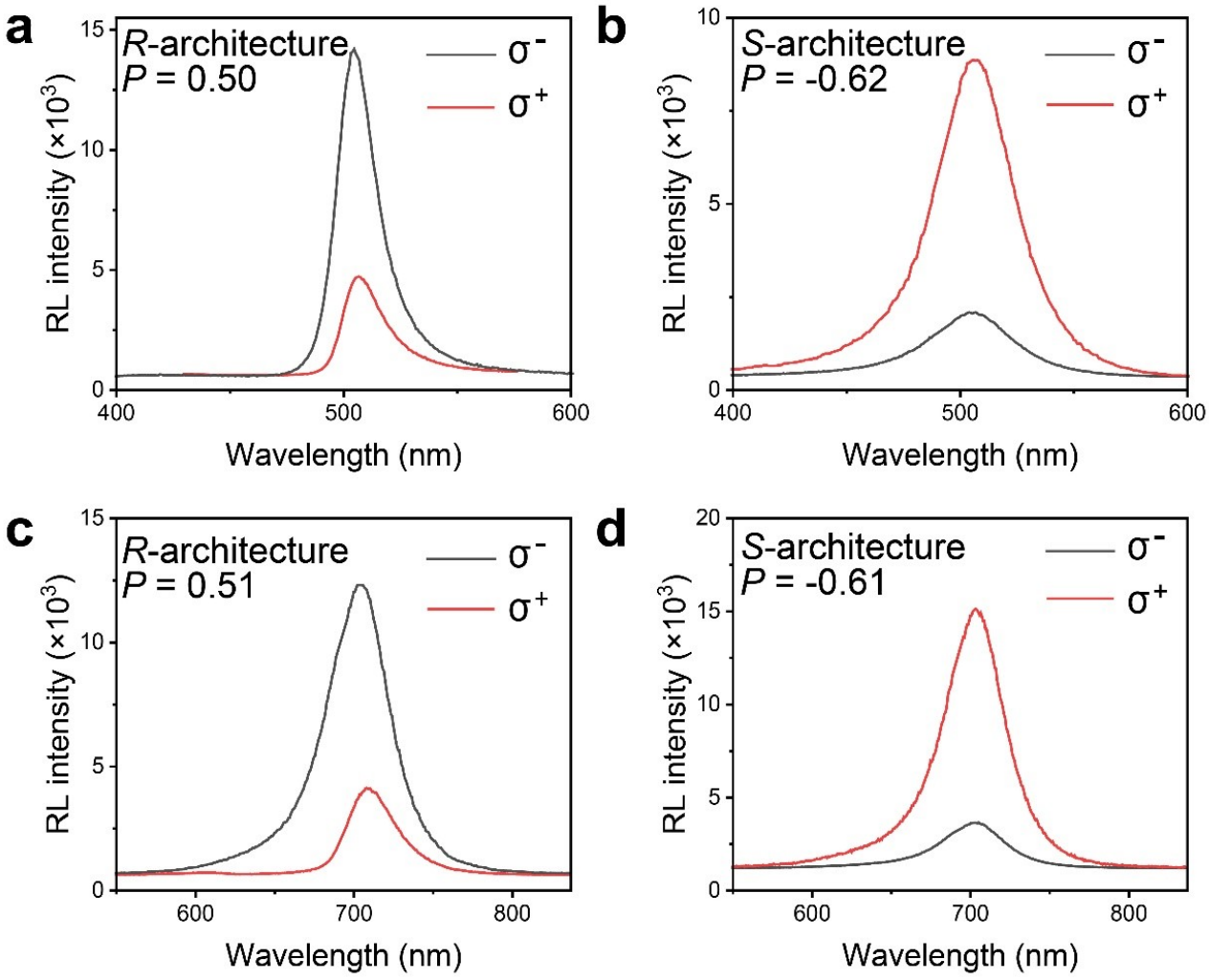

Figure S19. Polarization-resolved radioluminescence spectra and corresponding *P* values of (a) $FAPbClBr_2$-based *R*-architecture, (b) $FAPbClBr_2$-based *S*-architecture, (c) $FAPbBrI_2$-based *R*-architecture and (d) $FAPbBrI_2$-based *S*-architecture under X-ray excitation in a typical experiment.

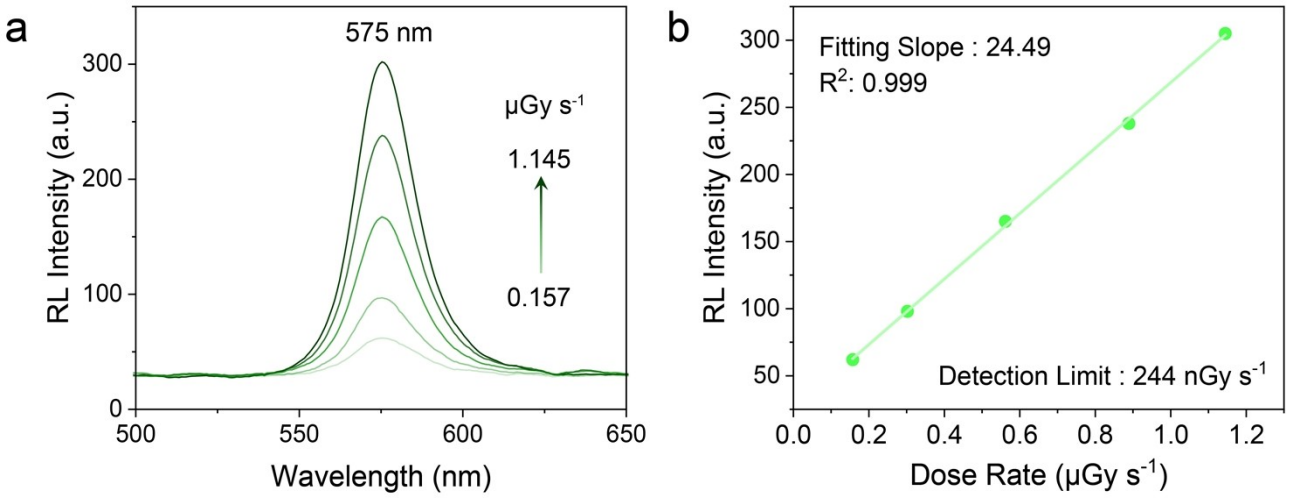

Figure S20. (a) Radioluminescence spectra of *S*-architecture under different X-ray dose rates; (b) X-Ray detection limit of *S*-architecture.

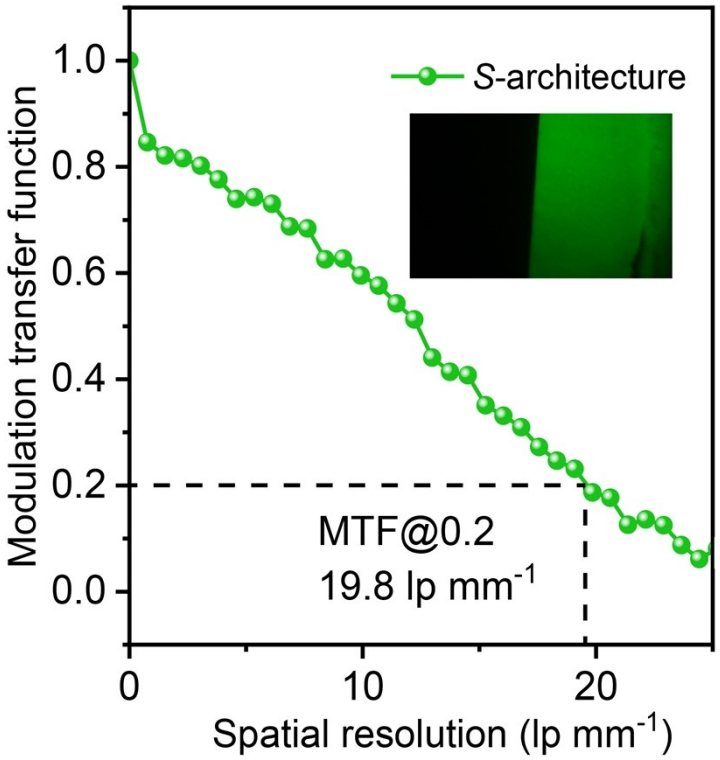

Figure S21. Modulation transfer function (MTF) of X-ray imaging (inset) obtained from *S*-architecture.

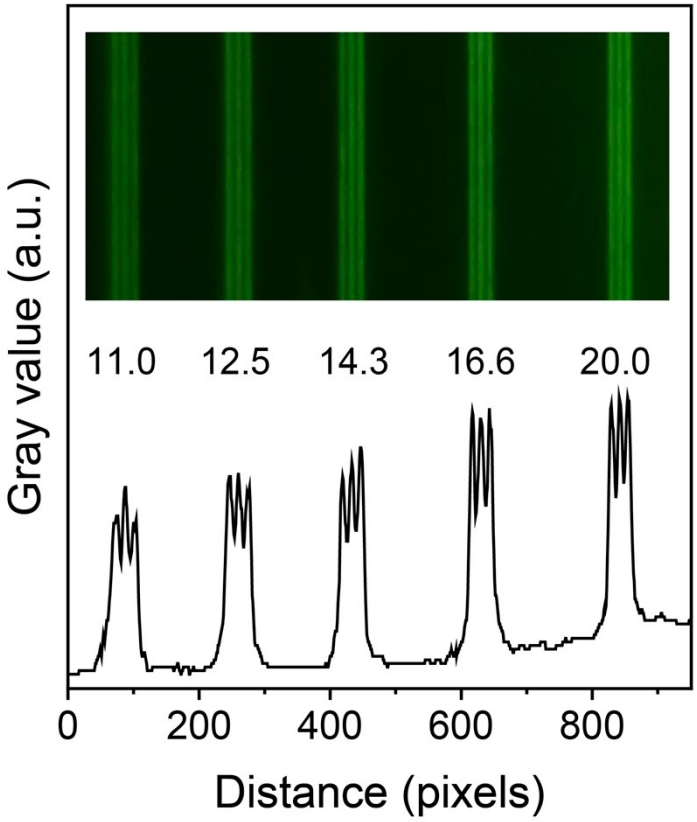

Figure S22. X-ray imaging of a standard resolution test pattern of *S*-architecture, showing resolved image resolutions from 11 to 20 lp mm^{-1}.

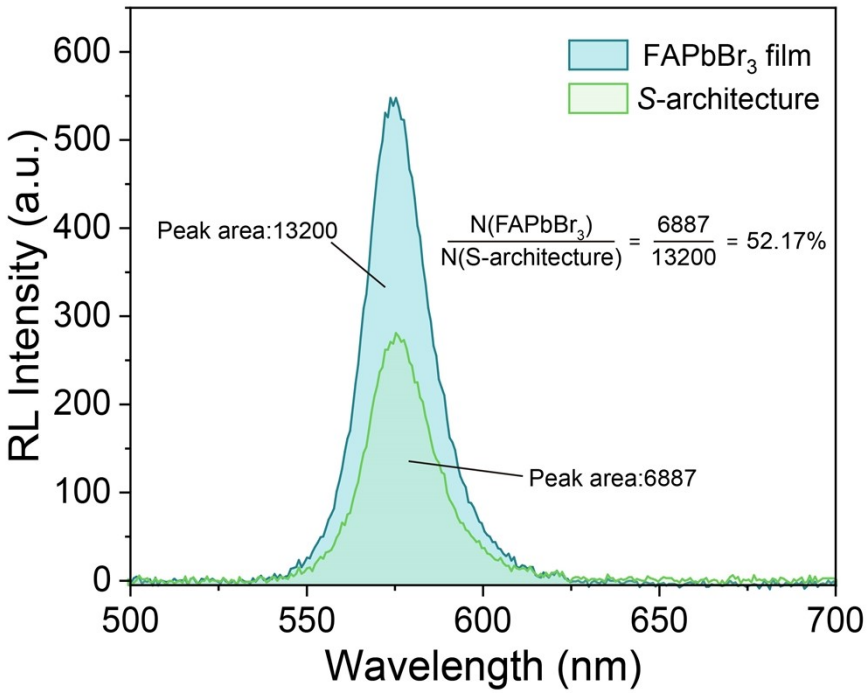

Figure S23. Radioluminescence (RL) spectra of $FAPbBr_3$ and *S*-architecture, measured under the same conditions. N($FAPbBr_3$) and N(*S*-architecture) denote photons counts of $FAPbBr_3$ and *S*-architecture, respectively.

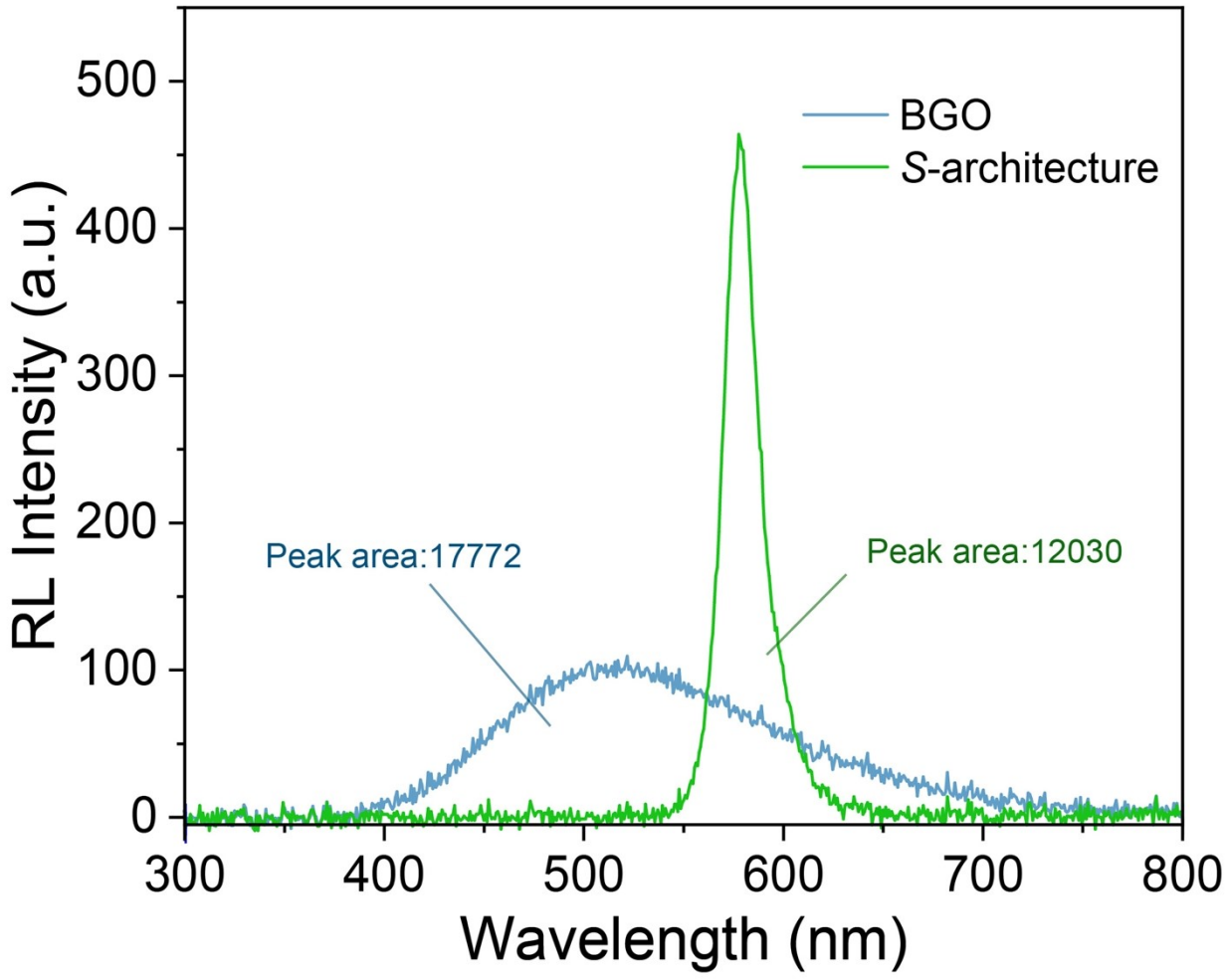

Figure S24. RL spectra of BGO and *S*-architecture, measured under the same conditions.

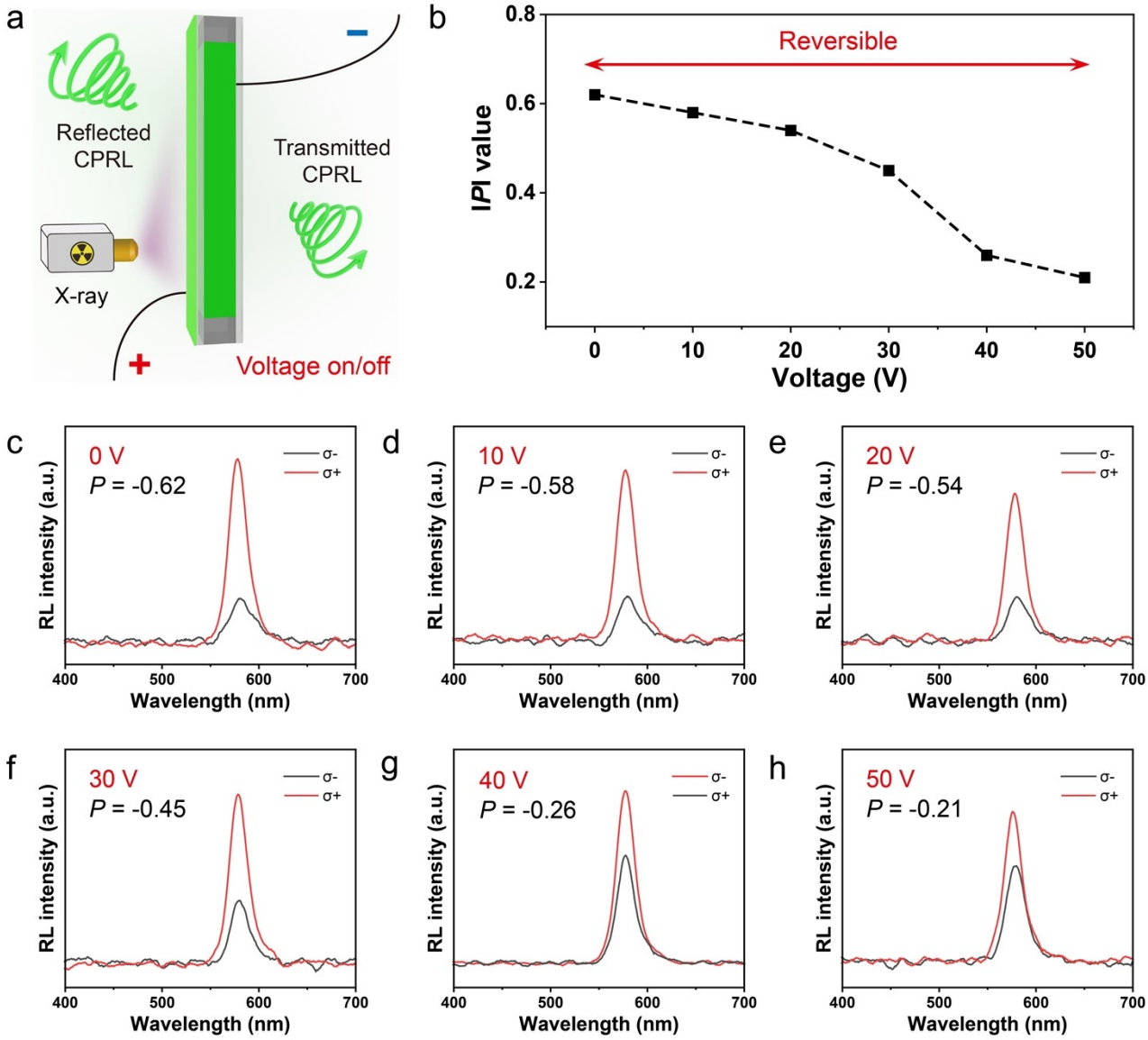

Figure S25. (a) Schematic illustration of CPRL generation from the chiral nanoscintillator architecture through the application of an external electric field. The cell was fabricated using ITO glass substrates. (b) The corresponding *P* as a function of the applied voltage, demonstrating reversible modulation. (c-h) Polarization-resolved radioluminescence spectra of an $FAPbBr_3$-based *S*-architecture under different applied voltages.